INTERNATIONAL ATOMIC ENERGY AGENCY
UNITED NATIONS EDUCATIONAL, SCIENTIFIC AND CULTURAL ORGANIZATION
INTERNATIONAL CENTRE FOR THEORETICAL PHYSICS
I.C.T.P., P.O. BOX 586, 34100 TRIESTE, ITALY, CABLE: CENTRATOM TRIESTE

UNITED NATIONS INDUSTRIAL DEVELOPMENT ORGANIZATION

INTERNATIONAL CENTRE FOR SCIENCE AND HIGH TECHNOLOGY

H4.SMR/544 - 8

Winter College on Ultrafast Phenomena

18 February - 8 March 1991

Creation of pico-and femtosecond light pulses by methods of nonlinear fiber optics

A. Karasik
General Physics Institute
Moscow, USSR

MAIN BUILDING STRADA COSTIERA, 11 TEL 22401 TELEFAX 224163 TELEX 460392 ADRIATICO GUEST HOUSE VIA GRIGNANO, 9 TEL 224241 TELEFAX 224531 TELEX 460449

Creation of pico-and femtosecond light pulses
by methods of nonlinear fiber optics.

A.Karasik
General Physics Institute,
117942 Moscow, USSR Vavilov street,38
Phone:132 83 76,Telex:411074 LIMEN SU

1. Introduction.

The creation of silica fibers with low optical losses initiated the development of several new directions of science and technology, i.e. fiber communication and fiber sensors. Recently, silica fibers attracted an attention as an object of nonlinear processes investigation. Localization of radiation field in small (some micrometers) cross-section of fibers core resulting in high density of radiation power and large length of radiation interaction with medium significantly increase the efficiency of nonlinear optical processes [1]. The fiber as an optical nonlinear medium has important peculiarities. The fiber limits the diffraction divergence of laser beam and forms its own mode fields which usually do not change their configuration at the whole length of waves interaction. It is possible to vary the number of modes in the necessary way altering some fiber parameters and to pass from mode statistics of multimode fiber to discrete number of modes of lowmode fiber and at last to singlemode fiber preserving high spatial laser coherence.

There are some remarkable properties of fused quartz: good transparency in visible and near infra-red spectral range from 0,4 to 1,8 μm, the presence of positive and negative group velocity dispersions (GVD) in this wavelength region, big number of overlapped broadband phonon resonances.

The nonlinear fiber optics gives new possibilities for control of spectral, spatial and temporal laser parameters. For example, we can tune frequency of laser radiation by using four-photon mixing and stimulated Raman scattering (SRS), we can restore a laser beam using phase-wave conjugation at stimulated Brillouin scattering. An important application of the nonlinear SPM and SRS and influence of GVD on processes in fibers occurs in the field of optical pulse compression and selection. Today pulse compressors on the base of fiber and grating pair are used in commercial laser systems. Soliton-pulse self compression opens another possibility for control of pulse duration and creation of fiber-Raman and soliton lasers.

In these lectures we shell discuss several nonlinear effects in fibers and methods of creation of ultra short pulses (USP). There are several methods on generation of ultra short pulses in

the pico- and femtosecond ranges, while controlling properties of radiation such as the amplitude and phase envelope, frequency and spectral composition.

2. Stimulated Raman Scattering, Group Velocity Dispersion and tunable picosecond pulses.

The creation of tunable USP sources in wide spectral region is an important problem for ultra fast phenomena physics. SRS in fibers opens new opportunities for construction of tunable converters of pico- and femtosecond radiation.

One of the most widely used materials which to a greater or lesser extent is subject to laser radiation is the glass. Studies of SRS in glasses are particularly important, especially from the point of view of the influence of SRS on lasing processes, particularly on generation of picosecond pulses in activated glass lasers. Intensive studies of SRS in glasses have started since the appearance of silica fibers with low optical losses which not only have made it possible to reduce the threshold power of process, but also to avoid self-focusing which splits a laser beam into filaments of higher power density and which makes it difficult to interpret the experimental results. At picosecond excitation GVD begins to play an important role in nonlinear processes because of its influence on the interaction length of different waves frequencies in long media.

Singlemode fiber is unique object for the study of GVD influence on SRS. Unique properties of singlemode fiber are based on preservation of high spatial coherence along great length, small threshold power of SRS. Due to this we can use our tunable picosecond pumping in IR region where GVD changes its sign from positive to negative (λ_0= 1,3 um). Wide spectrum of inhomogeneously broadened overlapping vibrational resonances of the fused silica gives excellent possibility for investigations [5].

Tuning the wavelength of 30 ps pump pulses propagating through 250 m fiber from 1,17 to 1,35 um from positive to negative GVD range we have discovered that the Stokes shift of Raman component is changed from 0 to 500 cm^{-1}. (Fig.1) This effect can be explained by variation of the effective interaction length of pump and Stokes waves (L_{eff}) due to dispersive divergence or walk off of different frequency pulses and correspondingly by transformation of the SRS gain increment.

In common case the effective length of interaction between the pump and Stokes waves is governed by the "divergence" length of the envelopes of their pulses

$$L_d\ (\lambda_p,\ \lambda_s) = \tau_p / |1/V(\lambda_p) - 1/V(\lambda_s)| \qquad (1)$$

Here, $V(\lambda_p)$ and $V(\lambda_s)$ are the group velocities of the pump and Stokes waves. The effective length of interaction

$$L_{eff}\ (\lambda_p,\ \lambda_s) = \begin{cases} L_d\ (\lambda_p,\ \lambda_s) & \text{for } L_d \leqslant L \\ L & \text{for } L_d > L \end{cases} \qquad (2)$$

It follows from (1) and (2) that L_{eff} is governed by the spectral dependence of the GVD and by the wavelengths λ_p and λ_s. Our fiber had zero GVD at $\lambda_o = 1{,}295$ µm, positive GVD in the range $\lambda < \lambda_o$, and negative GVD at $\lambda > \lambda_o$ (In principle it is possible to shift the value of λ_o changing parameters of fibers).

Calculated spectral dependencies of the SRS gains obtained from different λ_p (identified by arrows) as a result of multiplication of $g\ (\Delta\nu)$ and L_{eff} curves show their difference (Fig. 2). Maxima of these dependencies determine frequency shift $\Delta\nu$ of Raman components and correspond well with the experimental spectra.

We used the spectra in Fig.2 to determine for each pump wavelength λ_p the value $\Delta\nu$ at which the function gL_{eff} reached its maximum and this enabled us to plot the dependence of the shift of the Stokes $\Delta\nu$ relative to the pump line as a function of the λ_p (Fig. 3). The experimental points fitted well the calculated curve, thus confirming the model of the SRS discussed here and based on group delay effects.

3. Self-phase modulation and pulse selection.

3.1. SPM and spectral filtering.

Nonlinear process of SPM leads to Stokes-anti-Stokes spectrum broadening or frequency "chirp". This process is connected with nonlinear dependence of refractive index on the radiation intensity (I). Significant spectral broadening in bulk media is reached at condition of self focusing when laser beam in

media breaks down some filaments of self focusing. As a result we have nonmonothonic "chirp" for the whole cross section of laser beam and the compression of these pulses is not effective. Using single-mode fiber as nonlinear medium and realizing linear "chirp" for the whole profile of laser beam it is possible to get more than 100-fold one-stage compression of picosecond pulses.

For investigations of SPM we developed the method of spectral filtering. This method allows to study temporal characteristics of different radiation frequencies components and to form single pulses with smaller duration than the input one [6,7,8].

3.2. Self-phase modulation, Stimulated Raman Scattering and pulse selection.

The combined effect of SRS and SPM during the propagation of powerful light pulses in fiber can lead to generation a spectral continuum and to possibility of highcontrast pulse selection [6,7].

At SRS central part of a pumping pulse is converted in Stokes pulse . The central part of a pulse had a linear frequency sweep before the beginning of SRS. The SRS thus prevents an effective pulse compression in dispersive delay line. As a result of SRS we have two pulses or "fragments" which have a peak power $\sim P_{cr}$. (P_{cr} corresponds to the case in which the power level of the Stokes component at the fiber output is equal to the power level of the pump). An estimate of P_{cr} for singlemode 10m fiber yields ~ 1,5-2 kW. We can note that the "fragments" of the pump have a negative "chirp" (the frequency decreases toward the end of the pulse), and they undergo a self-compression in the region of the positive GVD ($\lambda < 1{,}33$ um). The fiber would have to be ≥1 km long for substantial compression of these "fragments".

As the peak power (P_{pump}) in the fiber is increased to a level slightly below that P_{cr} of SRS, the pulse spectrum is broadened to ~ 10 cm^{-1} by the SPM. As the pump power is raised further to $P_{pum} > P_{cr}$, the Stokes component of the SRS observed, shifted $\Delta\nu \sim 440\ cm^{-1}$ from the pump frequency. The onset of the SRS is accompanied by the simultaneous appearance of the intense spectral continuum. This continuum spreads out Stokes - anti Stokes ranges of hundreds cm^{-1} (The spectral density of the light at $\Delta\nu = 100\ cm^{-1}$ is 10^{-2} of the corresponding value at $\lambda = 1{,}06$

μm).

To find out the nature of the continuum we have measured the temporal characteristics of different spectral components by spectral filtering. Curve 1 in Fig. 4 shows autocorrelation function corresponding to the pump light. The dashed curve corresponds to the input 60 ps pulse. Curve 1 corresponds to the case of an efficient SRS. An autocorrelation function with three peaks corresponds to a pump pulse after its central part has been "eaten away" by the SRS. The time interval between two "fragments" depends on the extent which P_{pump} exceeds P_{cr}. The width of the central peak is ~ 30 ps and corresponds to a "fragment" duration ~ 20 ps.

Curves 2-5 (Fig.4) show function corresponding to the anti-Stokes components shifted 9,36,72 and 104 cm^{-1}, respectively, with respect to λ_{pump} with increasing $\Delta\nu$, the width of the central peak decreases, while the intensity of the side peaks falls off. The high contrast of the autocorrelation function (curve 5) indicates that the filtering of the light emerging from the fiber makes it possible to obtain a single pulse with τ_p= 2-3 ps.

As a result of investigations we find out that spectral continuum generation is explained by formation of steep fronts in the SRS and pump pulses as the pump pulse is eaten away by the SRS. These sharp fronts are formed at energy conversion from pump to Stokes. Fig.5 shows "Numerical oscillogramms" of SRS dynamics and of the nonlinear dynamics of frequency scanning in the pump pulse, computed for experimental situation including the influence of theGVD. The nonlinear dynamics of pump and Stokes pulses is determined by the exponential nature of Raman amplification: $I_S(z,\tau)$~ exp $[gzI_p(z,\tau)]$. For intensities I_p~ I_S, narrow spikes of intensity appear in the central pulse part and correspond to Stokes fluctuations spikes due to spontaneous Raman noises. Time duration of these spikes is determined by inverse broad width (~100 cm^{-1}) of spontaneous Raman spectrum of fused silica. These very short spikes determine very sharp pulse fronts. The abrupt phase jump takes place on this sharp front and produces large frequency shift and leads to the appearance of a broad spectral continuum. It follows from numerical calculations that spectral filtering with this kind of nonlinear frequency variation within

the pump pulse in the anti Stokes region relative to the pump can be used to select a single pulse. Horizontal lines in the lower part of the Fig.5 show the spectral regions of variations of the pump pulse frequency in which single pulses can be selected by spectral filtering.

We note that the dynamics of the generation of ultra short SRS pulses taking into account SPM and GVD is described by a set of nonlinear Schrodinger-type equations. These equations were exploited the "multiplication" of the initial frequency scanning range due to the SPM from pump to Stokes during the SRS generation.

4. Self-Induced SRS and Self-Compression of Pulses.

When the wavelength of the pump pulse falls in the negative GVD region of the fiber, both pump pulse and SRS created Stokes pulse can experience the soliton effects occurring as a result of common influence of nonlinear and dispersive effects. The theoretical treatments [12] show an interesting possibility of highly efficient nonlinear conversion of multisoliton pulse into singlesoliton Raman pulse from a monochromatic probe wave. The influence of self-induced SRS on propagation of singlesoliton was theoretically investigated [13], and it was shown that continuous Stokes shift of pulse frequency ω_0 took place. However, the author [13] did not consider the effects connected with dependence of the real part of the nonlinear cubic susceptibility ($\chi^{(3)}(\omega)$) on light frequency.

We discuss another approach [14]. The input pulse propagating as high-order soliton, narrows its width and broadens its spectrum. The spectrum of Raman amplification in glass is spread out practically from zero frequency shift. As a result, the blue components of the pulse pump the red components through self-induced SRS [18]. A pulse spectrum after SPM has a number of discrete Stokes-anti Stokes frequency components. We can consider the situation, when molecular vibrations of glass are excited by each pair of spectral components, when the difference of two frequencies is equal to phonon frequency (ω_{ph}).

$$\omega' - \omega = \omega_{ph} \qquad (4.1)$$

This process was experimentally investigated for fiber in [15].

The amplitude of molecular vibrations exciting by the difference ω' ω

$$Q(\omega_{ph}) \sim \int d\omega'_s E'^*_s(\omega'_s) E'(\omega'+\omega_{ph}) \qquad (4.2)$$

The excitation of molecular vibrations will be efficient, if the process is coherent and phases of all spectral components coincide. So, we must have the pulse without phase modulation. And on the contrary, molecular vibrations will be nonintensive, if the pulse has significant phase modulation.

It is possible to describe self-induced SRS in the following manner for the electrical pulse field $\sim \bar{e}E(t) \exp[-i(\omega_0 t - kz)]$. The contribution in nonlinear polarization, which is governed by vibrational resonances, is given by [16]

$$\bar{p}^{(3)}(t) = \bar{e}E(t) \int_0^\infty d\theta\, h(\theta) |E(t-\theta)|^2, \qquad (4.3)$$

where $h(\theta)$ is a function of time and characteristics of the material. The transformation pulse spectrum due to self-induced SRS is calculated carrying out Fourier-transform of Eq (4.3)

$$i(dE'(\omega)/dz) \sim -\int d\omega_{ph} \chi^{(3)}(\omega_{ph}) E'(\omega-\omega_{ph}) \int d\omega_s' E_s'^*(\omega_s') \cdot E'(\omega'+\omega_{ph}), \qquad (4.4)$$

where spectral pulse component -

$$E'(\omega) = \int_{-\infty}^{\infty} dt\, E(t)\, e^{i\omega t}, \qquad (4.5)$$

and

$$\chi^{(3)}(\omega) = \int_0^\infty d\theta\, h(\theta)\, e^{i\omega\theta} \qquad (4.6)$$

$Im\chi^{(3)}$ is proportional to Raman gain and determines the spectrum of Raman amplification. We can add Eq (4.4) to nonlinear Schrodinger equation and calculate the dynamics of pulse propagation at self induced SRS. $Im\chi^{(3)}(\omega)$ and $Re\chi^{(3)}(\omega)$ submit to Kramers Kronig relations [16] and the dependence of $Re\chi^{(3)}(\omega)$ can be calculated using the spectrum of Raman amplification $g(\omega) \sim Im\chi^{(3)}(\omega)$.

Note, that $Re\chi^{(3)}(\omega)$ is responsible of phase shift due to the SRS, and spectral dependence of $Re\chi^{(3)}(\omega)$ essential influences the pulse propagation dynamics.

The calculations [14] have shown that match and mismatch of phases of pulse spectral components depend on the sign of the GVD. In the region of the negative GVD ($k''<0$) the SPM and dispersion lead to creation of phase-modulated broadened pulse. As a result, self induced SRS is suppressed even at broad pulse spectrum.

Fig.6 shows the calculated dynamics of the envelope and spectrum of the pulse propagating single-mode fiber, as 3 order soliton for the negative GVD at enhancement of normalized propagation distance. At the enhancement of fiber length the extended Stokes wing appears in pulse spectrum and the extension of this wing is broader, than frequency shift between the pump and Stokes components of SRS at zero GVD ($\Delta\nu \sim 440$ cm^{-1}). An intense short pulse on the background of a broad pedestal is formed and it is preserved at fiber lengths significantly longer than selfcompression length of multisoliton pulse.

At spectral filtering of the Stokes wing the single pedestalless pulse is formed on the contrary of pulse at simple multi soliton compression.

These numerical results allow to interpret the results of experimental investigations, for example [17-19]. The review of works on soliton effects in SRS includes the book [1].

For the first time the phenomenon of self induced SRS was demonstrated in ref [18], where authors carried out the investigations of 30 ps pulse propagation into 250 single mode fiber in the negative GVD range (1,5-1,65 um). It was shown that the spectrum of radiation is symmetrically broadened due to the SPM at the fiber output, when the input pulse power is increased consequently from 50 up to 70 W (Fig.7). Because of the common effects of the SPM and the GVD at λ_p=1,54 um, the pulse begins to be compressed, forming an intense narrow spike on wide pedestal, according to the theoretical predictions [4]. This spike determines overall spectrum broadening. The part of broad spectrum falls into Raman amplification band of fused quartz leading to the formation of regular probe wave. This moment is accompanied by the appearance of Stokes wing in the spectrum (P_p=100 W). This wing contains about 50 % of all light energy at P_p=900 W.

The GVD plays important role in effective energy conversion. In this process the Stokes pulse is delayed relatively to pump pulse and "eats out" the trailing part of the pedestal of the pump pulse. As P_p is raised, the SRS appears earlier, and therefore the Stokes pulse can acquire more energy.

As a result of self-induced SRS the high contrast pedestal free Raman pulses with duration ~ 200 fs and peak power ~ 50 kW are formed in Stokes spectral range in contrast to pulse on pump frequency. It was possible to tune these pulses by means of the pump pulses tuning in the range of the negative GVD from 1,5 to 1,65 um. Thus, the nonlinear process of self-induced SRS gives the possibility to create high-contrast tunable femtosecond light pulses using initial picosecond pulses propagating single mode fiber in the negative GVD region.

List of Figures

Fig.1. SRS spectra of a single mode fiber 250 m long obtained on variation of the wavelength λp (identified by arrows) of pump radiation pulses (τp = 30 ps). Spectral resolution 6,3 nm.

Fig.2. Calculated spectral dependencies of the SRS gain increment obtained for different pump wavelength λp (identified by arrows).

Fig.3. Dependence of the frequency shifts of the Stokes components of SRS relative to the pump line calculated as a function of the λp using the data of Fig.2. The experimental points are superimposed on the graph (Ref. [5]).

Fig. 4. Autocorrelation functions of radiation at fiber output in the anti-Stokes region relative to the pump: 1 - $\Delta\nu = \nu a - \nu p$ = 0, 2 - 9 cm^{-1}, 3 - 36 cm^{-1}, 4 - 72 cm^{-1}, 5 - 104 cm^{-1}. The dashed curve corresponds to input pump pulse (Ref. [6]).

Fig. 5. "Numerical oscillogramms" of SRS dynamics (I_p, I_s) and of the nonlinear dynamics of frequency scanning in the pump pulse p(z, τ) in the fiber. τ_0 = 60 ps, the amplification SRS length $Zg = 2/GEp^2$, Z/Zg = 8 (a), 10 (b), 27 (c) (Ref. [7]).

Fig. 6. Dynamics of pulse envelope and spectrum Sw in fiber at λ = 1,55 μm, I_0 = $3,5 10^8$ W/cm^2, τ_0 = 1 ps, the dispersion length Z_d = τ_0^2/K'' = 22 m Z/Z_d = 0,05 (a), 0,0767 (b), 0,085 (c).
d - after spectral filtering for (c) (Ref. [14]).

Fig. 7. Pulse spectra of 30-ps input pulses at 1,54 μm propagated in the negative GVD of a 250 - m long fiber for four values of the input peak powers in the range 50-900W. Autocorrelation trace of the Stokes tail in the spectrum (900 W) (Ref. [18]).

References.

1. G.P.Agrawal, Nonlinear Fiber Optics, Acad. Press., Inc., 1989.
2. Ultra Short Pulses, Editby S.L.Shapiro Springer-Verlag Berlin Heidelberg, New York, 1977.
3. R.H.Stolen, in Optical Fiber Commun, ed. by S.E.Miller and A.G.Chynoweth, New York, 1979, Chap. 5.
4. L.F.Mollenauer, R.H.Stolen, J.P.Gordon, W.J.Tomlinson, Opt. Lett. 8, 289, 1983.
5. E.M.Dianov, L.M.Ivanov, A.Ya.Karasik, P.V.Mamyshev, A.M.Prokhorov, Sov. Phys. JETP 64(6), 1205 (1987).
6. E.M.Dianov, A.Ya.Karasik, P.V.Mamyshev, G.I.Onischchukov, A.M.Prokhorov, M.F.Stel'makh, A.A.Fomichev, JETP Lett. 39, Nc 12, 691, 1984.
7. E.M.Dianov, A.Ya.Karasik, P.V.Mamyshev, A.M.Prokhorov, V.N.Serkin, Sov.Phys. JETP 62 (3), 448 (1985).
8. E.M.Dianov, L.M.Ivanov, A.Ya.Karasik, P.V.Mamyshev, A.M.Prokhorov, JETP Lett, 44, No 3, 155 (1986).
9. B.Nicolaus et.al. Opt. Lett. 8, 189 (1983).
10. A.M.Weiner et.al. Opt.Lett. 11, 153 (1986).
11. A.S.L.Gomes, A.S.Gouveia-Neto, J.R.Taylor, H.Avramopulos, G.H.C.New, Opt. Comm. 59, 399 (1986).
12. V.A.Vysloukh, V.N.Serkin JETP Lett. 38, 199 (1983).
13. J.P.Gordon Opt. Lett. 11, 662 (1986).
14. E.A.Golovchenko, E.M.Dianov, A.Ya.Karasik, P.V.Mamyshev, A.N.Pilipetskii, A.M.Prokhorov Sov. Quantum Electronics 16, N 3, 592 (1989).
15. T.T.Basiev, E.M.Dianov, E.A.Zakhidov, A.Ya.Karasik, S.B.Mirov, A.M.Prokhorov JETP Lett 37, 229 (1983).
16. R.W.Hellwath Proc.1 Sov-Amer Symp.M.,270(1970)
17. E.M.Dianov, A.Ya.Karasik, P.V.Mamyshev, G.I.Onishchukov, A.M.Prokhorov, M.F.Stel'makh, A.A.Fomichev JETP Lett 39, 691 (1984).
18. E.M.Dianov, A.Ya.Karasik, P.V.Mamyshev, A.M.Prokhorov, V.N.Serkin, M.F.Stelmakh, A.A.Fomichev JETP Lett 41, 294 (1985).
19. P.Beaud, W.Hodel, B.Zysset, H.P.Weber JEEE J.Quantum Electron QE 23, 1938 (1987).

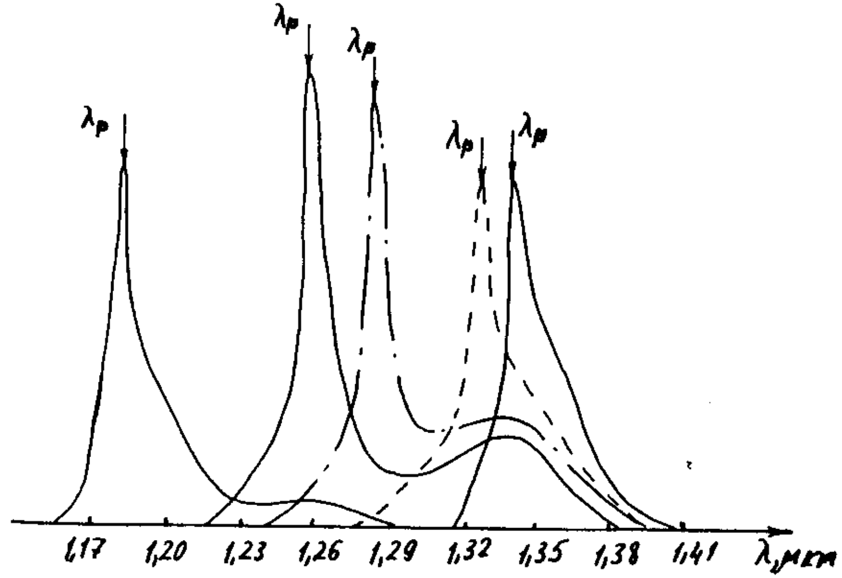

Fig. 1

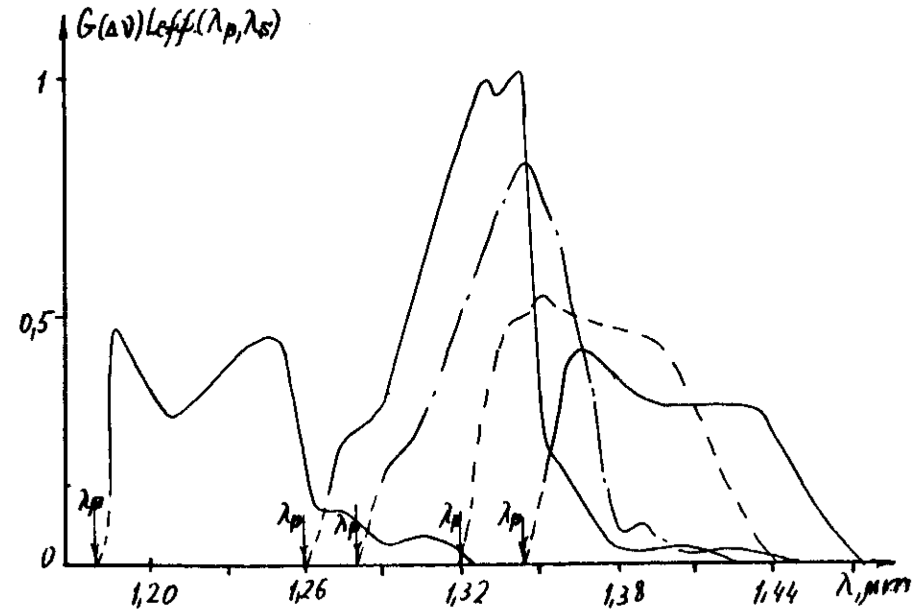

Fig. 2

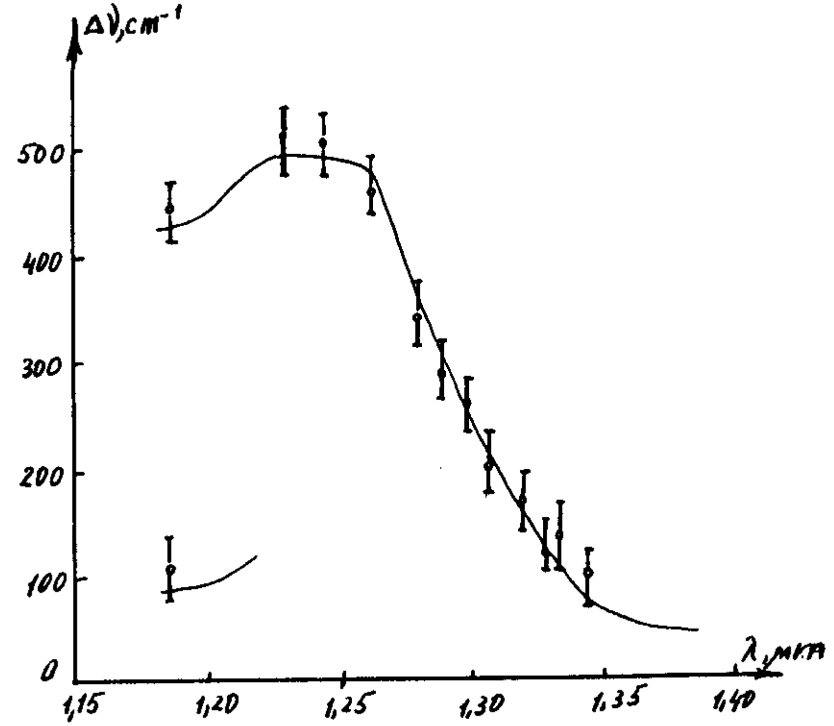

Δν, cm⁻¹
500
400
300
200
100
0
1,15
1,20
1,25
1,30
1,35
1,40
λ, mkm

Fig. 3

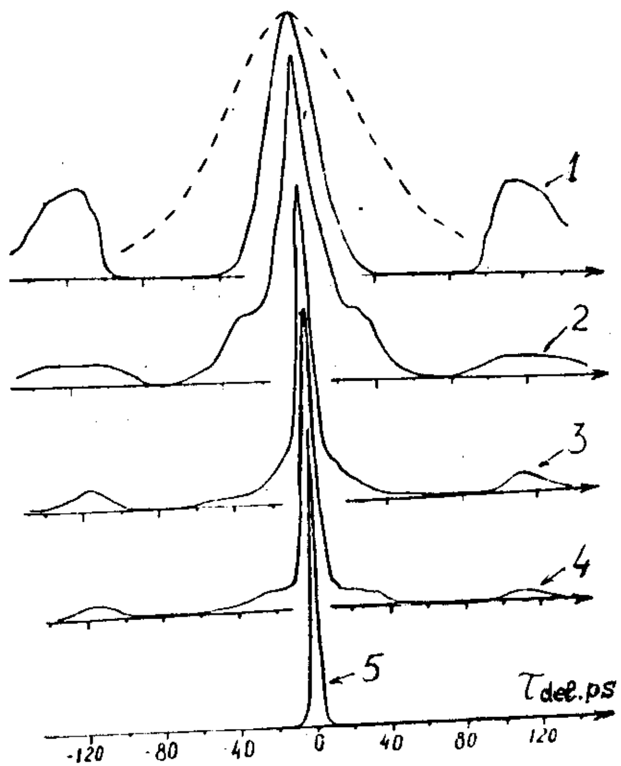

1
2
3
4
5
τdel.ps
-120
-80
-40
0
40
80
120

Fig. 4

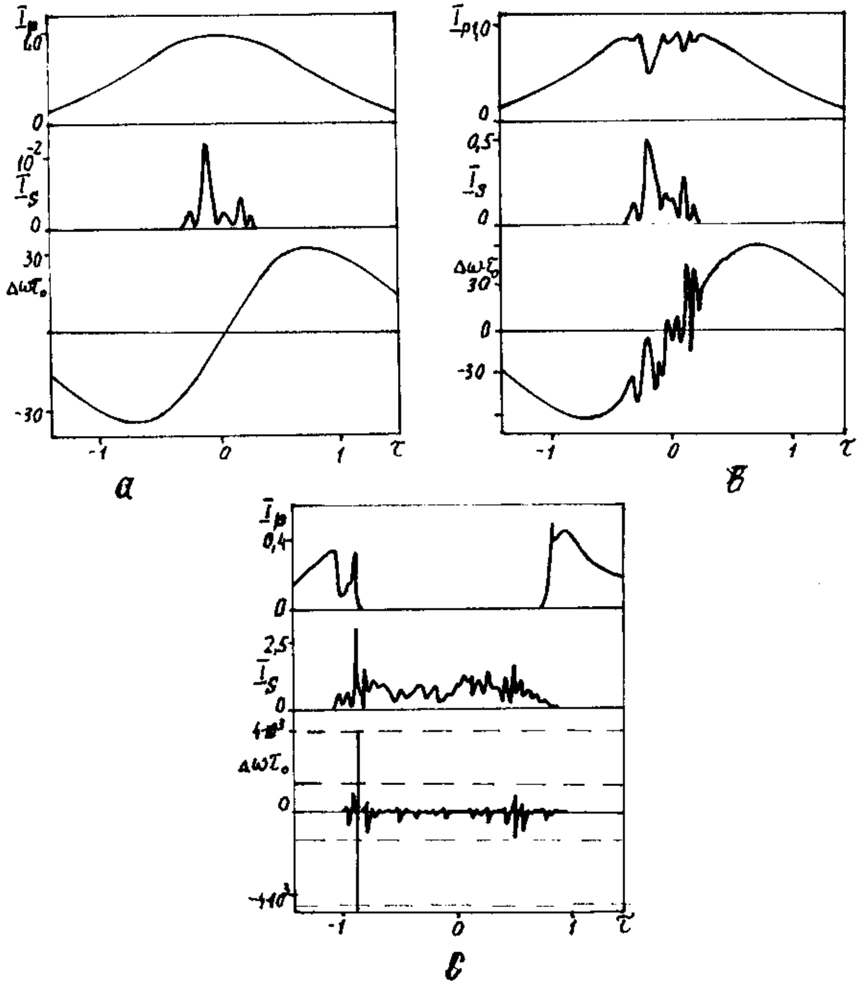

$\bar{I}_p$
1,0
0
10^{-2}
$\bar{I}_s$
30
$\Delta\omega\tau_0$
-30
-1
0
1
τ
a
0,5
б
0,4
2,5
в

Fig. 5

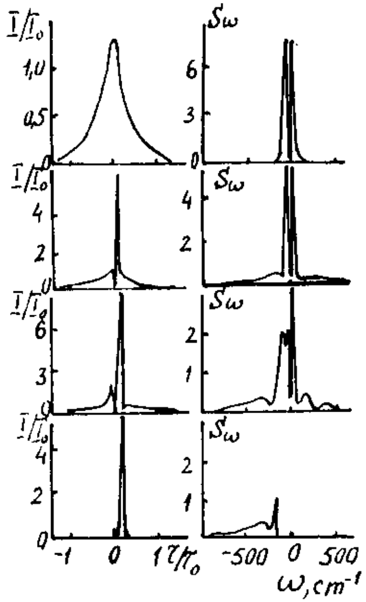

$\bar{I}/\bar{I}_0$
S_ω
1,0
0,5
0
6
3
4
2
-1
1
τ/τ_0
-500
500
ω, cm^{-1}

Fig. 6

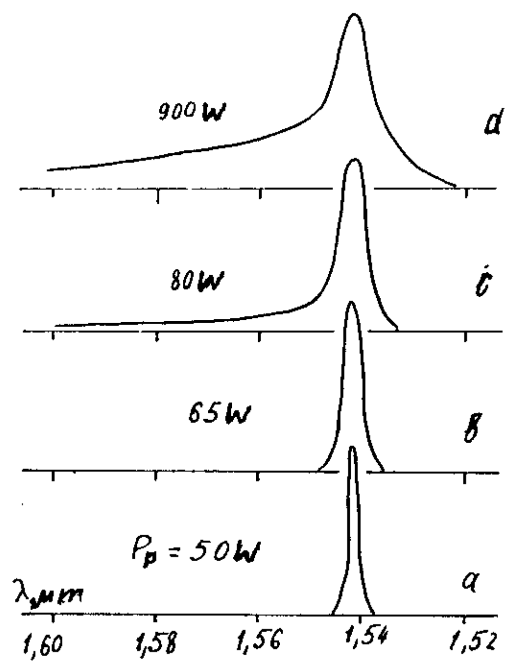
900W
d
80W
c
65W
b
P_p = 50W
a
λ,μm
1,60
1,58
1,56
1,54
1,52

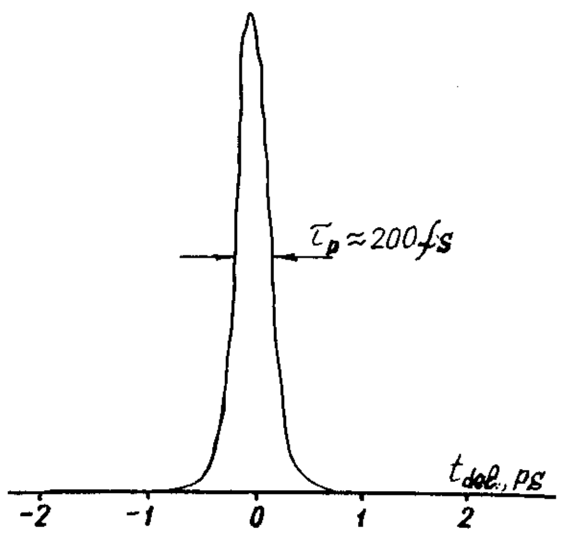
$\tau_p \approx 200fs$
$t_{del.}$, ps
-2
-1
0
1
2

Fig. 7